GEOPHYSICS, VOL. 82, NO. 5 (SEPTEMBER-OCTOBER 2017); P. B165–B176, 11 FIGS.
10.1190/GEO2017-0153.1

Case History

The impact of magnetic viscosity on time-domain electromagnetic data from iron oxide minerals embedded in rocks at Opemiska, Québec, Canada

Frédéric E. S. Gaucher[1] and Richard S. Smith[1]

ABSTRACT

The magnetic viscosity (MV) effects observed at time scales between 0.01 and 10 ms at Opemiska are associated with magnetic grains of variable size in rocks. Recent observations made during a ground time-domain electromagnetic (TDEM) survey at Opemiska are consistent with four aspects of the spatial and amplitude characteristics of a MV response: (1) the $\partial B_z/\partial t$ decay rate is roughly proportional to $1/t^{1+\alpha}$, where $-0.4 < \alpha < 0.4$, (2) the anomalies are mainly visible on the z-component, when the EM receiver sensor is located inside or just outside the transmitter loop, (3) there is no obvious x- or y-component response, and (4) the sites where MV effects are seen in the TDEM data are coincident with an airborne magnetic anomaly. Previous studies have demonstrated that MV could be caused by (1) fine-grained particles of maghemite or magnetite in the overburden, regolith, or soil that were formed through lateritic weathering processes, (2) volcanic glass shards from tuff containing approximately 1% by weight magnetite, which occur as grains approximately 0.002–0.01 μm in size precipitated in a spatially uniform way, or (3) from the *Gallionella* bacterium that precipitates ferrihydrite that oxidizes to nanocrystalline maghemite aggregates. The sites investigated at Opemiska are outcropping and well-exposed with relatively little or no overburden, and they are unfavorable for the formation of maghemite; hence, it is assumed that the source of MV seen at Opemiska cannot be the maghemite, or the other aforementioned causes. Hand samples were collected from Opemiska to identify the minerals present. Polished thin sections observed under an optical reflecting microscope identified the accessory minerals magnetite, ilmenite, and pyrrhotite, all known for their relatively high magnetic susceptibility. The use of the scanning electron microscope confirmed fine-grained magnetite grains as small as 0.667 μm. An electromagnetic induction spectrometer confirmed the viscous nature of the susceptibility of the Opemiska samples. This suggests that MV could originate not only from fine-grained magnetite and maghemite particles located in the weathered regolith but also from other iron oxides and magnetic minerals embedded in the rock itself.

INTRODUCTION

Magnetic viscosity

Magnetic viscosity (MV) is an effect exhibited by fine-grained magnetic minerals that gradually align atomic spins to develop an induced magnetic field oriented with an external magnetic field. The same effect can be observed when there is a change of the exciting field, or there can be a decay in the induced field when the external magnetic field is removed (Barsukov and Fainberg, 2001; Dunlop and Özdemir, 2001; Pasion et al., 2002). The phenomenon is also called superparamagnetic (SPM) effects, frequency-dependent, or time-dependent magnetic susceptibility.

Rock magnetism researchers (Néel, 1949; Stacey, 1962; Stacey and Banerjee, 1974; Hodych, 1977; Halgedahl and Fuller, 1980; Boyd et al., 1984; Williams and Dunlop, 1989; Worm et al., 1991; Xu and Dunlop, 1993; Dunlop, 1995) have found that magnetism in minerals can occur in domains in which the spins are aligned in parallel or antiparallel directions and magnetic minerals can either

Manuscript received by the Editor 9 March 2017; published ahead of production 13 May 2017; published online 06 July 2017.
[1]Laurentian University, Harquail School of Earth Sciences, Sudbury, Ontario, Canada. E-mail: fred@goldmanexploration.com; rssmith@laurentian.ca.

contain multiple domains (MD) or single domains (SD). Extremely fine-grained magnetic minerals (slightly <1 μm) tend to have an SD and realign their atomic spin with a relaxation time on the order of milliseconds, so they behave viscously (Dunlop and Özdemir, 2001). In a multidomain grain, the individual domains may reorient the grain's magnetic direction (Bogdanov and Vlasov, 1966), or even enlarge some of the domains at the expense of others (Stacey and Banerjee, 1974; Dunlop, 1995). These multidomain grains tend to hold their magnetization for much longer periods. Rather than exhibiting a sudden transition between SD and MD, there seems to be a smooth transition between the two behaviors (Stacey, 1962; Fabian and Hubert, 1999).

Our research aimed to explain the MV seen at Opemiska with a timescale of observation between 0.01 and 10 ms, corresponding to the time windows of the 15 or 30 Hz base frequency used during the time-domain electromagnetic (TDEM) survey. In this paper, we briefly review the influence of size and shape of magnetite grains on MV, and the environments in which MV has been detected. In the case of Opemiska, we characterize the MV decay using a decay rate for predictive mapping. We also investigate hand samples using petrophysical, optical, and scanning electron microscopic studies. Finally, we use an electromagnetic induction spectrometer to investigate the frequency dependence of the susceptibility to see if this is consistent with MV.

Size and shape of magnetite grains

Depending on the time of exposure to a magnetic field, MV is more pronounced in the SD range (0.1–5 μm), even though it can be substantial in the multidomain range (10–15 μm) (Parry, 1965; Dunlop, 1983). Mullins and Tite (1973) also report that the multidomain grains do display MV, with a response two orders of magnitude less that the SD grains. Dunlop and Schutts (1979) demonstrate that viscous magnetization is strongest in SD grains of the order of 0.5 μm in size, but in the time scales of interest, it can also be appreciable in larger grains (10–15 μm) if they are elongated, a result consistent with the theoretical model developed by Butler and Banerjee (1975).

Buselli (1982) reports that the presence of fine-grained particles of magnetite with radii of the order of 0.025 μm or less, will cause these materials to exhibit magnetization and to behave viscously. Strangway et al. (1968) come to a similar conclusion for spherical magnetite or maghemite with grains of 0.02 μm for a 1 ms measurement at room temperature. Dunlop (1973) measures MV on equant grains ranging from 0.01 to 0.065 μm in size. Magnetic SD structures were observed on perfect octahedral crystal of magnetite by Özdemir and Dunlop (1993). However, Dunlop (1995) shows that magnetite grains as large as 10–100 μm in size can also have intermediate or pseudo-SD properties. Fabian and Hubert (1999) suggest that an imbalance in asymmetrical particles contributes substantially to the SD-like fraction of the overall remanence. Finally, Macnae (2016) suggests that the MV will be favored with grain sizes in the range of 0.1–0.9 μm and emphasizes that a preferred magnetization will be developed along the longest direction of the SD grains, aligned with the direction of the applied field, and that it is those grains that are causing detectable MV. Although there is some debate about the exact grain size and nature of the magnetic material causing the MV, it also appears that the grain shape, mineralogy, intensity of the field used to induce the remanence, and direction of the external field applied in regard to the axis of the grains are influencing the amplitude of the response obtained (Levi and Merrill, 1978).

Detection of magnetic viscosity

MV has been previously observed by different authors in (1) weathered oxidic soils of tropical and subtropical climates such as regolith in Australia (Buselli, 1982; Barsukov and Fainberg, 2001) and Africa (Macnae, 2016), (2) microcrystals of iron oxides in quenched volcanic glass shards from tuff, where approximately 1% by weight magnetite occurs as grains approximately 0.002–0.01 μm in size precipitated in a spatially uniform way (Schlinger and Smith, 1986; Schlinger et al., 1986; Julian et al., 1988; Dunlop, 1995), (3) airborne EM data from Greenland (Legault et al., 2016; S. Taylor, 2016, unpublished data), (4) attributed to fine-grained volcanic materials (Macnae, 2016), (5) associated with glacial tills in Finland (Montonen, 2015), and (6) from biogenic origin when *Gallionella* bacterium precipitates ferrihydrite that oxidizes to nanocrystalline maghemite aggregates (Moskowitz et al., 1988; Tabbagh and Dabbas, 1996; Konishi et al., 2012).

MV can be detected with decay constants in the millisecond range (Kratzer et al., 2013) using ground or airborne TDEM methods with a coincident loop TDEM configuration (Kozhevnikov and Antonov, 2011). In ground measurements, MV is mostly seen inside the loop, or a few meters outside (Buselli, 1982). In airborne measurements, MV signals decrease rapidly with height (Lee, 1978; Raiche, 1978; Buselli, 1982) and disappear in modern systems (where the receiver is inside the transmitter) if terrain clearances of approximately 50 m are reached (S. Taylor, 2016, unpublished data). This is intuitively reasonable because effects are most likely to be observed in cases, in which the applied field from the transmitter magnetizes material in close vicinity and the receiver is also nearby to sense these fields. The low-amplitude, slow decays caused by MV have a similar signature to good conductors, such as massive sulfides, and many anomalies have been previously misinterpreted as first priority targets to be drilled (Mutton, 2012; Legault et al., 2016; S. Taylor, 2016, unpublished data). Magnetically viscous minerals exhibit late-time power law decays with $V(t) \sim 1/t$ during the off time for an impulse response (Billings et al., 2003), and on a double logarithmic scale, the graph of $V(t)$ is a straight line with a slope of -1 (Buselli, 1982). This temporal behavior has also been observed by Nagata (1961), Barsukov and Fainberg (2001), Montonen (2015), and S. Taylor (2016, unpublished data), and explained mathematically by Chikazumi and Charap (1978), as cited in Lee (1984b).

METHODS AND RESULTS

Magnetic viscosity in TDEM field survey at Opemiska

During summer 2015, 14 different sites were investigated on the Opemiska property with ground fixed loop TDEM system using a square waveform. Out of the 14 sites investigated, 5 of them (sites #1, 4, 5, 10, and 12) were presumed to be exhibiting MV that shared the following characteristics:

1) The $\partial B_z/\partial t$ decay curve exhibits a negative slope with an approximate $1/t$ time dependence during the off-time, consistent with work from Buselli (1982), Lee (1984a), and Billings et al. (2003). However, the MV decay rate is sometimes slightly different from the $1/t$ time dependence. Observations show that the electromagnetic field transient response V in the receiver

sensor is proportional to $1/t^{1+\alpha}$, where $-0.4 < \alpha < 0.4$ (Figure 1). This observation is comparable with data collected by Barsukov and Fainberg (1997) and Sattel and Mutton (2014), where they observe $-0.2 < \alpha < 0.2$, and with data collected by Dabas and Skinner (1993), where they observe a power law with exponent −1.4 between 56 and 417 μs.

2) The relation of $V(t) = 1/t^{1+\alpha}$ is observed for the stations located inside the fixed ground loop transmitter and less than 10 m outside the edge of it (Figure 2). This observation is in agreement with Buselli (1982).
3) The TDEM anomalies attributed to be caused by MV are visible on the z-component, with no corresponding x- or y-component response (Figure 2). This observation is consistent with S. Taylor (2016, unpublished data).
4) All z-component profiles along the lines surveyed exhibit a similar shape. This profile shape is similar to the one also observed by Mutton (2012). There is a characteristic reversal of sign when crossing the loop edge, from inside the loop to outside the loop. The shape of the MV profile is similar to the monitored primary field at the receiver, but the amplitude of the MV response is several orders of magnitude smaller.
5) All the sites where MV was observed coincide with strong airborne magnetic field anomalies (Keating et al., 2010; Gaucher, 2017). This confirms the existence of magnetic material in the study area.
6) The overburden thickness is different at each site, ranging from zero to several meters of till, or tailings. Out of the five sites where the possible MV was observed, two of them had the survey equipment lying directly on outcrop (sites #1 and #4). On the other three sites (#5, #10, and #12), drilling confirmed 3–10 m of overburden before reaching bedrock. The decay regression analysis for the sites with the presence of overburden, confirmed negative slopes with systematic time dependence close to $1/t$.

Predictive mapping of mineralization using the α parameter

Barsukov and Fainberg (2001) show that in some cases, an MV effect can be used as a powerful exploration tool for certain types of mineral deposits. Their results show that for deep intrusive nickel orebodies, the parameter $\alpha > 0$ from $V(t) = 1/t^{1+\alpha}$ would indicate the location where ore deposits associated with magnetite exist, and $\alpha < 0$ indicates where there are not any orebodies.

At Opemiska, the α parameter from $V(t) = 1/t^{1+\alpha}$ was plotted for every TDEM station surveyed where MV was observed. Kriging interpolation of the $1 + \alpha$ parameter suggests a correlation between a large positive α and the chalcopyrite ore associated with magnetic minerals (shown with the black outline in Figure 3). The trend direction of the red zone corresponds roughly with the direction of the vein, but the sampling is poor; hence, the trend direction is not estimated with confidence. Further petrographic work and denser sampling are required to correlate α with chalcopyrite percentages and the direction of mineralization.

Petrophysical measurements on hand samples from Opemiska

At sites #1 and #4 where MV was observed in the TDEM data, outcropping bedrock allowed for rock samples to be collected for petrophysical and microscopic observations (Figure 4). Magnetic susceptibility measurements were done using the handheld multiparameter probe manufactured by Instrumentation GDD Inc. The magnetic susceptibility measured from the 10 samples collected at sites #1 and #4 ranges from 1.47 to 493×10^{-3} SI and is presented in Figure 4. The measurements were collected from hand specimens, from which the polished thin sections (PTSs) were also prepared. Because the coil of the handheld instrument is bigger than the rock samples, the measurements are considered only as semiquantitative, and they roughly indicate the range of magnetic susceptibility values. Microscopic observations confirmed the presence of magnetite grains in all the samples. The magnetite modal percentage was approximated by doing visual observations on PTSs, with content ranging from 1% to 15%.

Scanning electron microscope study

Objectives and methodology

Optical microscope examination of PTSs coming from Opemiska outcrops, in which MV was observed with the TDEM survey, shows obvious magnetite grains with diameters of less than 5 μm (Figure 5). These observations happen to be at the lower limit of the optical microscope used with a 40× lens. Ilmenite and pyrrhotite were also observed in these samples, and these minerals might possibly be contributing to the MV. Ilmenite lamellas were observed in the {111} planes of the host magnetite and chalcopyrite (Figure 6), and this oxyexsolved process (Lindsley, 1991) is known for subdividing the large grains into several magnetically independent smaller grains (Graham, 1953). Strangway et al. (1968) point out that the trellis texture of ilmenite lamellas may result in SD grains, with a grain diameter much larger than the SPM critical size calculated by the Néel theory. To confirm the finer grain structure of the magnetic grains,

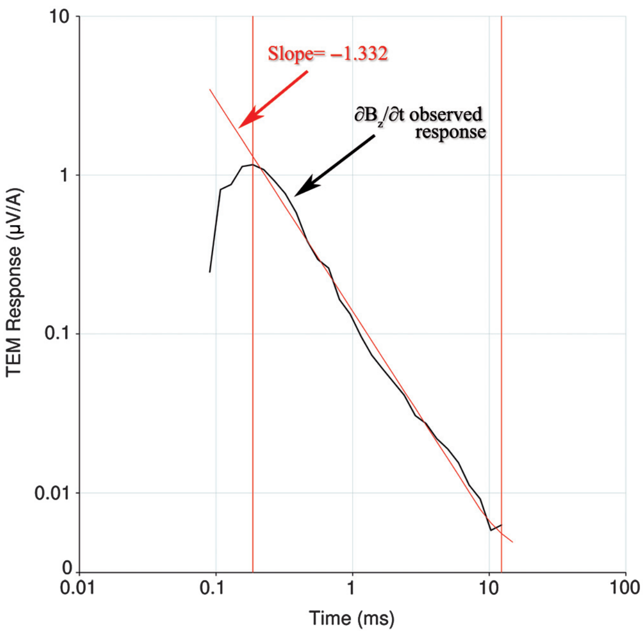

Figure 1. Linear regression analysis of the TDEM $\partial B_z/\partial t$ decay for the site #1, line 0, station −5 m. The TDEM $\partial B_z/\partial t$ decay linear regression line in red fitting the observed response in black exhibits a negative straight slope of −1.332 on a log-log scale.

a scanning electron microscope (SEM) was used to determine the accurate dimension (width) of the smallest iron oxide grains that could be observed. Four PTSs have been selected for SEM observations: PTS B and C from site #1, and PTS J and M from site #4.

The PTSs were first coated with carbon (0.015 μm thickness) prior to the observations under the JSM-6400 scanning microscope in the central analytic facility at Laurentian University in Sudbury. The voltage applied was 20 kV, with a current of 1 nA. Work conducted on the PTSs mainly used the back-scattering electron images (AUX) to locate and identify different minerals and obtain their respective chemistry by looking at their reference peaks. Mapping analysis has also been conducted for some areas of interest to evaluate all the elements that were present. Because the beam of the SEM used has a diameter of approximately 1 μm, the chemistry of the

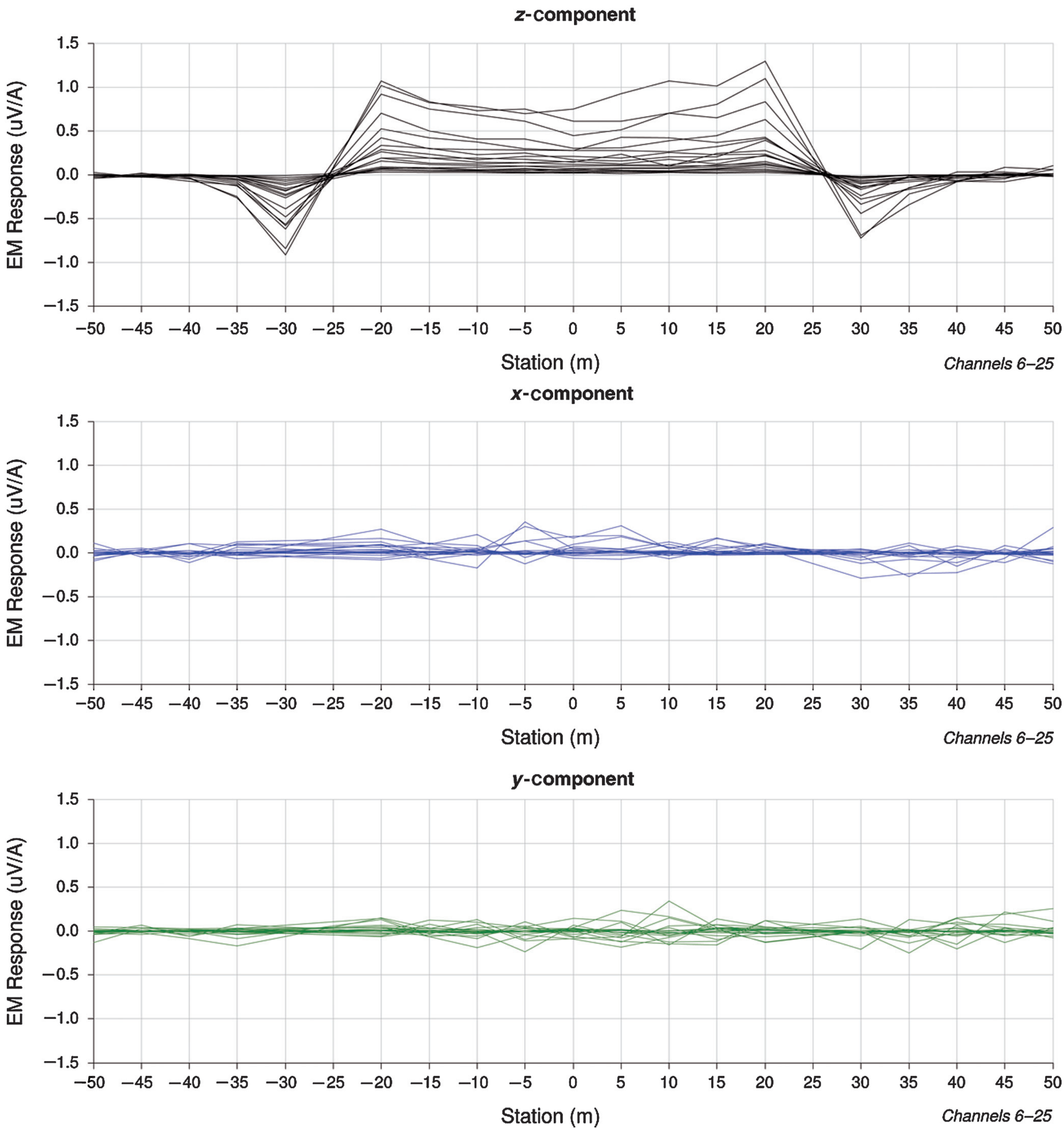

Figure 2. Profile response of the x-, y-, and z-components for site #5, line 0, at a base frequency of 30 Hz. The TDEM anomalies attributed to be caused by MV are visible on the z-component, with no corresponding x- or y-component response.

grains observed smaller than that dimension will encompass an average of the minerals surrounding them.

Results and interpretation from the SEM work

A magnetite grain with a grain width of 0.667 μm (Figure 7) was observed on the PTS J. All four PTSs examined under the SEM showed magnetite with grain widths as small as approximately 1 μm. The smaller magnetite grains are inferred to be the result of bigger grains that were broken. This grain fragmentation is interpreted to have developed during regional compression, which created folds and fractures, controlling the emplacement of the Cu-Au mineralization (Lavoie, 1972; Watkins and Riverin, 1982; Leclerc et al., 2009). Hence, one possible factor contributing to MV observed at Opemiska is the deformational history, which is partly responsible for the various sizes and orientations of the domains of the magnetite grains found in the rock samples.

EM induction spectrometer study

To confirm the possibility that MV was originating from the fine particles of iron oxides embedded in the Opemiska rock formations, an additional experiment was designed to observe the induced magnetic moment in laboratory-scale samples.

Principles of operation

The instrument used was the University of Toronto EM Induction Spectrometer (UTEMIS), a transportable tabletop instrument for measuring the ratio of the time-varying magnetic moment induced in small, laboratory-scale samples by a time varying, spatially uniform, alternating magnetic field. Static magnetic induction and eddy current induction are measured and expressed as the magnetance $\mathscr{m}$ of the form

$$\mathscr{m} = p_m/H, \tag{1}$$

where p_m (Am^2) is the induced magnetic moment and H (A/m) is the exciting magnetic field intensity. The ratio $\mathscr{m}$ has units of cubic meters, indicating the measurement is proportional to the sample volume (Bailey and West, 2007). However, the results of this study are normalized by the mass m, to give the magnetic mass susceptibility $\chi = \mathscr{m}/m$, as a way to account for the different shape and sample sizes. The mass susceptibility is thus expressed in units of $\mu\mathrm{l/g}(=10^{-6}\ \mathrm{m^3/kg})$. Volume could have been used as an alternative to mass normalization, but the relative effort and error in measuring mass was judged to be less than estimating volume. The UTEMIS reports its measurements of magnetance as a complex number, with the measurements given directly as real and imaginary components at a prescribed set of frequencies between 140 Hz and 63 kHz (West and Holladay, 2014).

To speed up the measurements, the applied field is not a single pure harmonic. The current that excites the Helmholtz configuration source coils of the system is generated from a prerecorded digital sequence 3 s long, consisting of six quasisquare-wave signals. Individual odd harmonics are extracted from the recorded signals

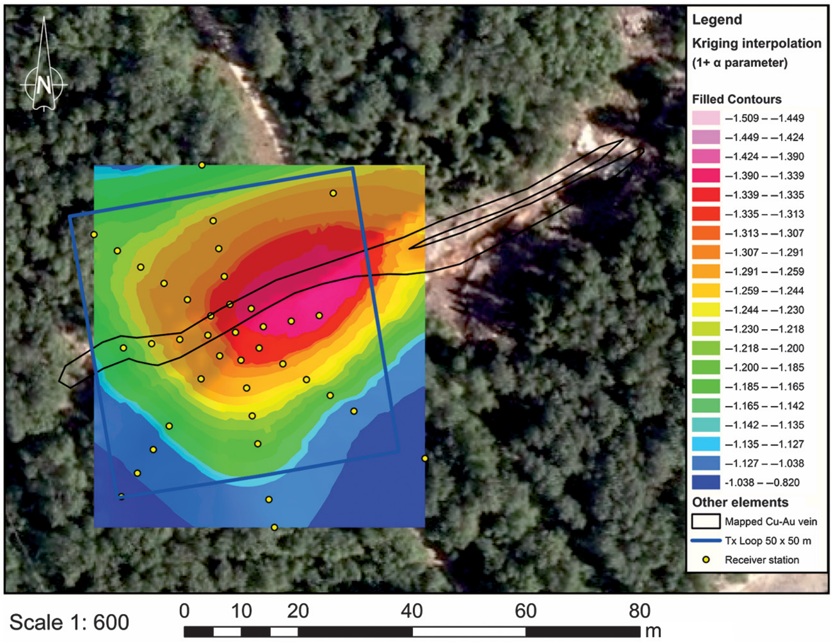

Figure 3. Kriging interpolation of the $1 + \alpha$ parameter, from the z-component, at site #1.

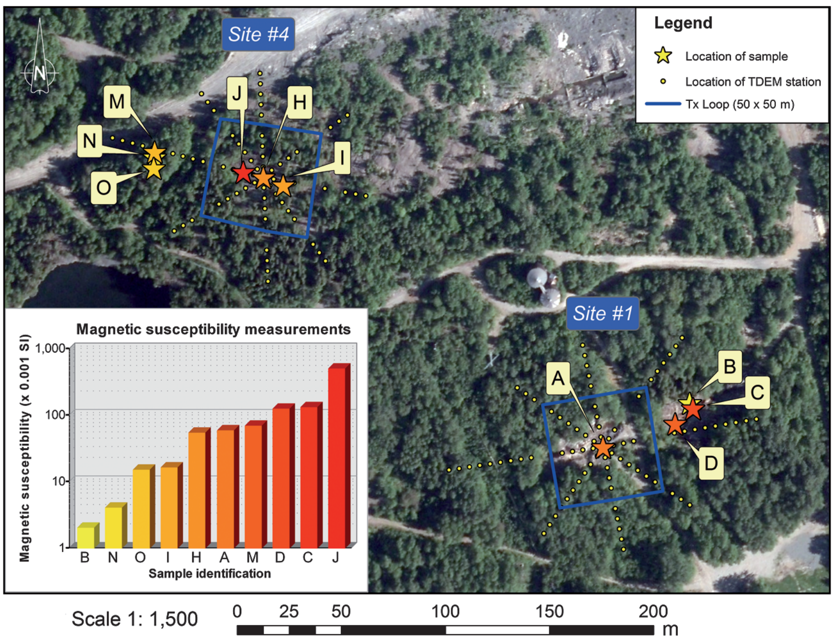

Figure 4. Location of rock samples used to prepare the PTSs and conduct the UTEMIS measurements on sites #1 and #4. Magnetic susceptibility measurements on the samples collected at sites #1 and #4 are also shown in the inset. The colors of the different stars represent the amplitude of the magnetic susceptibility measurements.

by Fourier analysis. The prerecorded sequence can be transmitted several times and stacked sequentially. Averages and standard deviations of the readings are calculated and the results are tabulated (Bailey and West, 2007). Figure 8 shows a picture of the mark II version of the UTEMIS and a close-up of a sample.

Methodology

Surface grab samples or diamond drill cores from Opemiska sites where TDEM surveys were done during the summer of 2015 were cut into rock cubes with dimensions of 2.5 cm or smaller to fit the vial of the UTEMIS. The 22 samples studied with the UTEMIS are the same samples used for the PTS study and correspond to a wide variety of Cu-Au veins, mineralization type, and host rocks. For statistical purposes, several rock-cube specimens coming from each site were prepared. The dimension of 2.5 cm or less ensures the magnetic field induced on the samples is as uniform as possible. We acquired four repeat measurements with the UTEMIS, except when the size of the sample was smaller than 2.5 cm, then 16 repeats were performed. This is because smaller sample volumes yield less signal, increasing the effects of noise and drift, particularly for weakly responsive samples (West and Holladay, 2014).

To ensure that the UTEMIS instrument was working properly, a calibration reading over a ferrite bead, and a copper loop were taken at the beginning and the end of the day. Figure 9a shows the pure inductive response from a copper loop wire with a zero in-phase response at low frequency and a quadrature response that peaks at the same frequency that the in-phase shows an inflection. The measurements from a nonconductive nonviscous but susceptible ferrite bead sample (Figure 9b) show a zero-quadrature response and an in-phase measurement that does not vary from the low-frequency value.

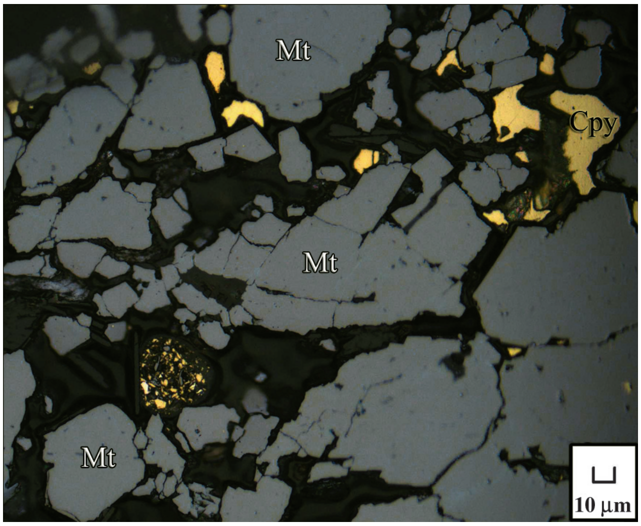

Figure 5. Optical microscope observation of PTS J (site #4). The magnetite grains appear broken into smaller pieces. Some of the magnetite grains have a diameter of less than 5 to 10 µm.

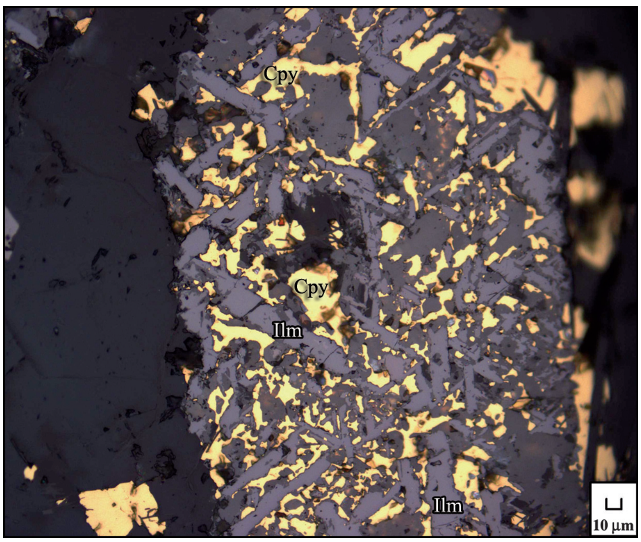

Figure 6. Optical microscope observation of PTS C (site #1). The ilmenite trellis texture presents broken edges with microcavities. It is interpreted that the ilmenite developed along the {111} planes of the magnetite and has subsequently been replaced by chalcopyrite.

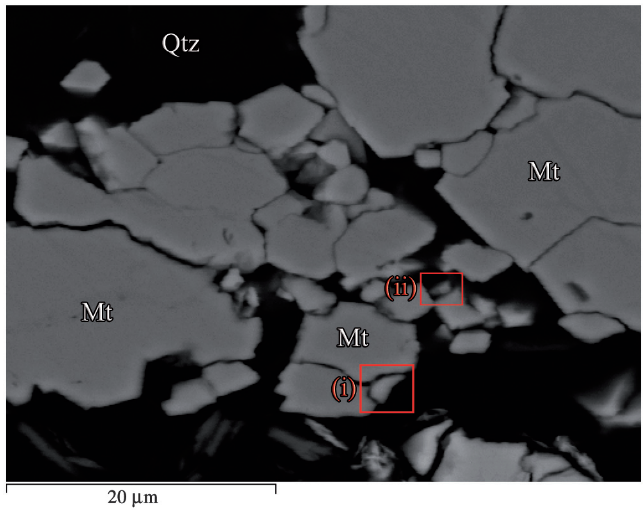

Figure 7. The SEM observation of PTS J (site #4). The magnetite grain width in (i) is 1.17 µm and in (ii) is 0.667 µm.

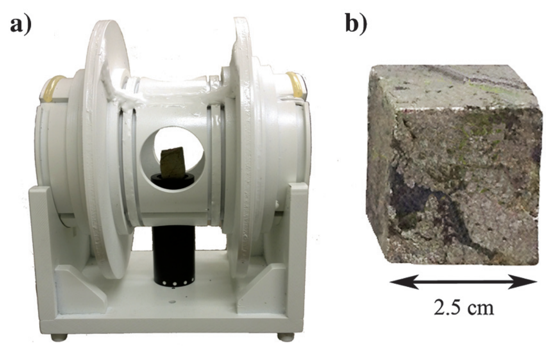

Figure 8. (a) Picture of the UTEMIS II with a pseudocubic 2.5 cm width specimen from Opemiska on the sample pedestal inside the instrument. (b) Close-up of cubic specimen from which UTEMIS measurements were made.

Samples that show viscous magnetization (Figure 9c) are expected to have an in-phase magnetization that decreases as frequency increases, with a nearly constant out-of-phase component (Das, 2005; Bailey and West, 2007).

Electromagnetic induction measurements results

Opemiska ore consists of semimassive to massive chalcopyrite, silver, and gold with erratic distributions of pyrite-pyrrhotite-magnetite. The veins and veinlets are hosted in a gabbro with quartz, calcite, carbonate, and stilpnomelane (McMillan, 1972). Opemiska rocks exhibit a wide range of physical properties, chemical composition, mineralogical assemblages, and textures. The responses obtained with the UTEMIS reflect this variety and are presented in Figure 10. The type of responses obtained from Opemiska rock samples can be summarized into four main categories:

1) A response exhibiting a constant relatively small magnetization for the in-phase component, with an obvious out-of-phase response displaying a negative slope (Figure 10a). The highest frequency response shows no appreciable in-phase component, and the largest observed out-of-phase response was measured at −3.55 μl/g for the 63 kHz frequency. The inductive limit is not reached, taking into account that higher frequencies are not measured. This spectrum, with variation in the out-of-phase component only, suggests the presence of a weak to moderate conductor. The small but invariant in-phase component suggests a small amount of ferromagnetic material with frequency-independent susceptibility.
2) A moderate to strong magnetization response visible on the in-phase component, with no out-of-phase component (Figure 10b). The susceptibility spectrum for the in-phase component shows almost no dispersion and is constant. This suggests the presence of ferromagnetic material with coarse grains, with multidomain boundaries and no frequency dependence or MV.
3) A stronger negative slope in the in-phase component in comparison with the other samples, with a corresponding negative peak in the out-of-phase component (Figure 10c). One interpretation is that this frequency-dependent magnetization response suggests the presence of a conductor, with the in-phase component representing the induction of conduction currents (eddy currents) superposed on a frequency-independent induced magnetization. In this case, the sample contains material that is conductive and multidomain ferromagnetic. The mineralogical microscopic observations confirm the presence of pyrrhotite, chalcopyrite, and magnetite, which may explain the UTEMIS response. On the other hand, there is ambiguity and the spectrum might indicate a strong change in the susceptibility as a function of frequency, which will distort the in-phase component and the out-of-phase components as a consequence of the Kramers-Kronig relation.
4) A negative slope in the in-phase component, with a constant negative out-of-phase component (Figure 10d). This type of response in which the spectrum exhibits dispersion infers MV: The in-phase component declines with a proportional increase in frequency with a steady negative out-of-phase. A Kramers-Kronig relationship between the in-phase and quadrature was expected to be visible (Van Kampen and Lurçat, 1961). However, the expected decline in the out-of-phase response predicted from the changes in the in-phase is not seen. The standard deviation

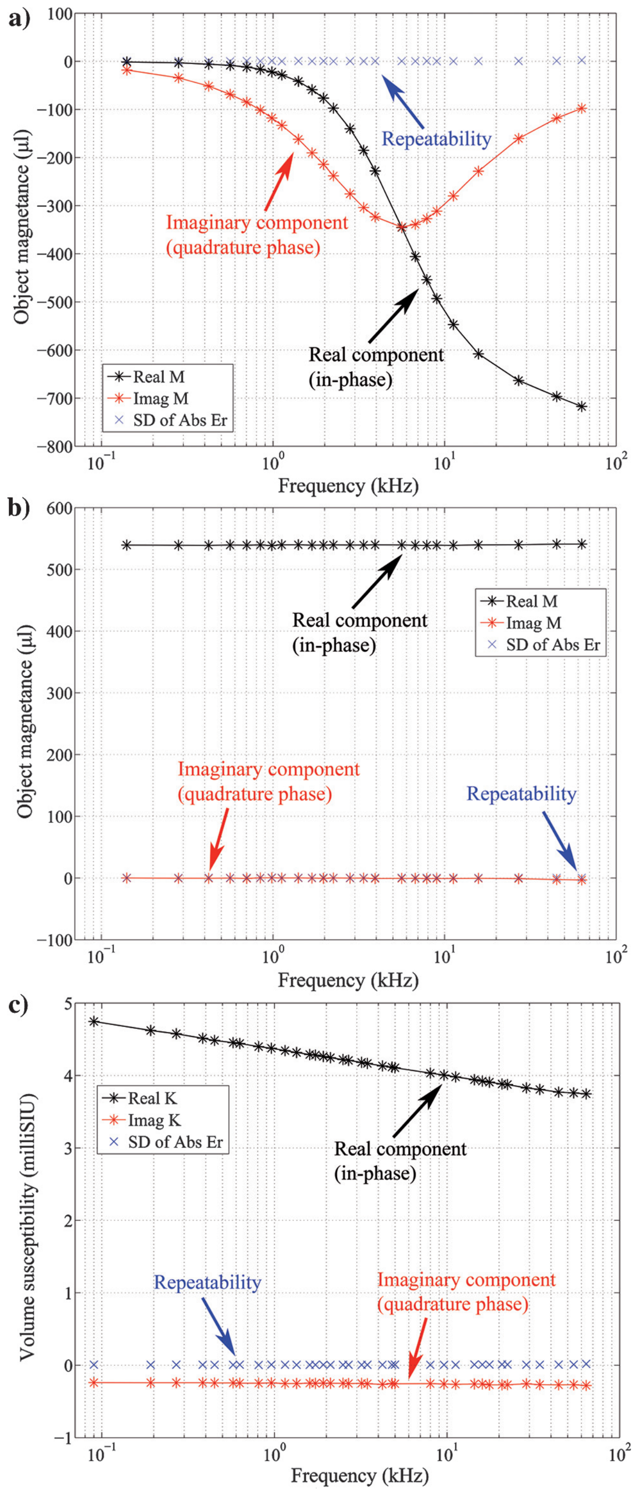

Figure 9. Plots of UTEMIS responses for the frequency spectrum of magnetance obtained for known samples. The magnetance was not normalized by the mass for panels (a and b), and normalized by volume for panel (c). (a) Conductive sample with no magnetic susceptibility (copper ring sample). (b) Magnetic susceptible sample with no conductivity and no MV (ferrite bead sample). (c) Soil sample from Australia (AzC-2, 12.5 ml), exhibiting MV. The in-phase component varies as a function of frequency, and it declines as the frequency increases, whereas the out-of-phase component is negative and approximately constant (modified from Bailey and West, 2007).

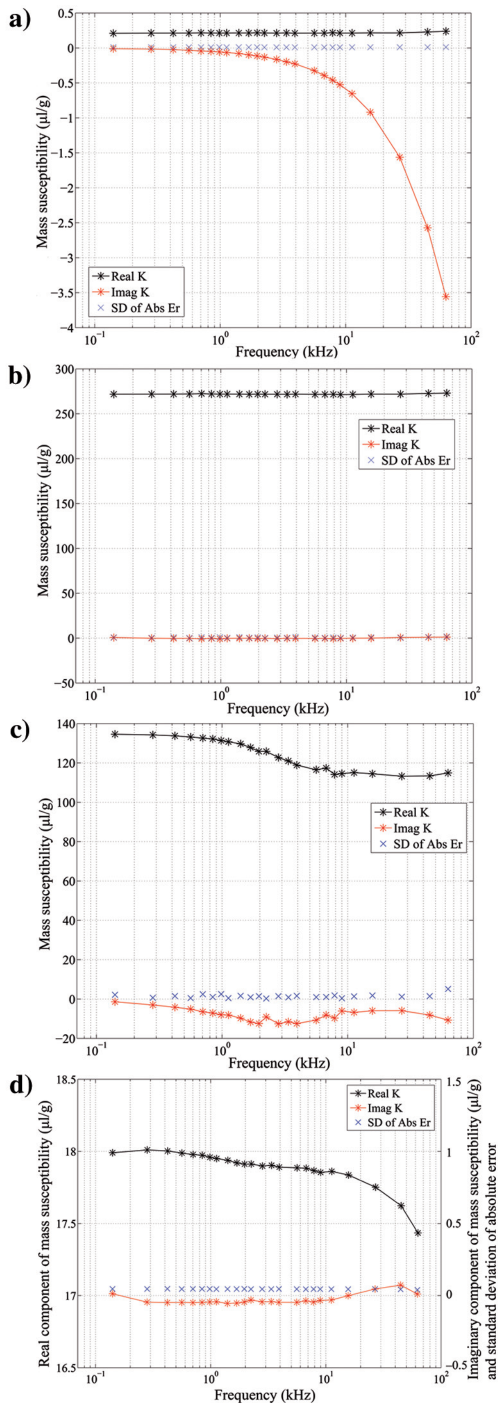

Figure 10. Plots of UTEMIS responses for the frequency spectrum of mass susceptibility obtained from Opemiska rock samples: (a) Weak conductive material with very weak magnetic susceptibility (sample B4, 42.9 g). (b) High magnetic induction material with no conductivity (sample F1, 3.7 g). (c) A frequency-dependent magnetization response showing a strong negative slope in the real component, with a corresponding quadrature component (sample R1-repeat, 1.9 g). (d) A frequency-dependent magnetization response showing a negative slope in the real component, with a nearly constant negative imaginary component (sample J4-ii, 16.5 g). The in-phase decline over a 0.5 μl/g interval is proportional with the increase in frequency, and it shows a dispersive spectrum typical of MV. The anomalous measurements values at low and high frequencies may be affected by extraneous sources.

error is 0.05 μl/g, 10 times less than the declining interval 0.5 μl/g observed for the in-phase component.

DISCUSSION

Coarse-grained magnetite is typically nondispersive (Bailey and West, 2007). Measurements with the UTEMIS on Opemiska rock samples show a wide range of magnetization amplitudes, sometimes with a weak frequency-dependent response superposed. This suggests that magnetic material embedded in the rock is comprised of coarse and fine grains. The coarse multidomain grains will amplify the magnetization response, whereas the fine SD grains will be time dependent and decay with time.

The observations made with the spectrometer are consistent with the PTS studies. For example, the PTS J for which MV seems to be observed with the UTEMIS has been described with a modal composition consisting of 65% chalcopyrite, 15% magnetite, 15% quartz, 5% pyrite, and traces of biotite. Looking at this specific PTS under the microscope, one can clearly see that some of the largest magnetite grains appear to have been crushed as a consequence of the physical strain, resulting in smaller very fine broken grains. Qualitatively, the grain size is not uniform and spreads over at least four orders of magnitude. The SEM study on PTS J confirmed the size of magnetite grains to be as small as 0.667 μm. Thus, it is possible that very fine magnetic grains (<1 μm) would induce a response different from large ones (>100 μm) as suggested by previous workers, and that these two responses would be superimposed. Even though the modal abundance could be determined quantitatively, it is interpreted that this wide range of grain sizes lead to an induced magnetization superimposed with a MV. The volume fraction of coarse ferromagnetic grains in the rock will enhance the strength of the magnetization and exhibit a susceptibility that is frequency independent, whereas the fine magnetic grains show a viscous magnetization, and exhibit a frequency dependence.

These induction measurements, done independently from the PTS and SEM studies, support the a priori hypothesis that MV could be seen in the z-component response from the Geonics coil sensor used during the 2015 field TDEM survey at Opemiska. The slow $\partial B_z/\partial t$ decay amplitude measured inside the TDEM loop for the vertical component exhibited a $1/t$ dependence, and it was seen between 0.2 and 7 ms at 30 Hz. PTS J comes from the TDEM site #4 investigated during the 2015 summer, where MV is hypothesized to be observed. The UTEMIS measurements done on PTS J, showed a frequency-dependence visible from 140 Hz to 63 kHz. This frequency spectrum range corresponds to the equivalent of the time range that the TDEM instrument is sensitive to.

Other hypotheses were examined to attempt to explain the slow z-component decay that could originate from another source than the magnetic minerals embedded in the rock itself:

- A slow leakage of the TDEM transmitter after the turn-off, potentially resulting in a residual current flowing in the ground after the nonideal termination. However, two different transmitters were used, manufactured by two different companies, GDD and Geonics, and the results were similar. It is unlikely that both instruments are at fault in an identical way. Also, similar effects were not seen at other resistive sites, suggesting a geologic explanation, not an instrument problem. If the shape of the late-time EM response is identical to the primary field, this would mean that the source of the signal is geometrically the same as the source of the primary field. The differences in shape between the primary field from the transmitters and their respective secondary response for late-time were examined closely by superimposing them at the same scale. The result shows that they are similar but do not fit perfectly. This would suggest that the signal seen is modified in some way by the magnetic field of currents induced at early time, or by some other current flowing in the ground.

- Another explanation could be magnetically viscous fine-grained particles of maghemite or magnetite in the overburden. However, some of the sites where the phenomenon was observed were surveyed with the TDEM sensor lying directly on the bedrock. There is bedrock alteration associated with mineralization at Opemiska, but this is limited to no more than twice the width of the associated mineralized veins (Watkins and Riverin, 1982), meaning a maximum of 3–5 m in total. The observed MV phenomenon was seen over an area of 50 × 50 m while surveying inside the loop. In addition, the climatic conditions in Québec for the last few thousands of years do not favor the formation of regolith as seen in tropical or subtropical soil environments. Even though oxidation of magnetite to maghemite is common but not abundant in North America, it has been observed in Canadian iron formations as a rim, sharp linear features, or masses within the magnetite grains (Mcleod, 1970). Maghemite is also observed in Canada in the oxidized zone of surface geologic deposits, and it is attributed to biochemical oxidation of pyrite (Pawluk, 1971). It is also sometimes inherited from the transformation of goethite during bush fires (Schwertmann and Fechter, 1984; Anand and Gilkes, 1987; Stanjek, 1987) or attributed to pedogenic processes (Van der Marel, 1951; Oades and Townsend, 1963; Taylor and Schwertmann, 1974). However, the Opemiska vein copper-gold deposit is interpreted to have been formed by hydrothermal process crosscutting a mafic to ultramafic sill (McMillan, 1972; Hutchinson, 1982; Salmon, 1982; Robert, 1994), and maghemite was not recognized in the PTS nor the SEM studies done on Opemiska rocks. Although further research is required to confirm the absence of maghemite in the soil at Opemiska, it is unlikely that altered magnetite present in the overburden at Opemiska could be the main source for the MV.

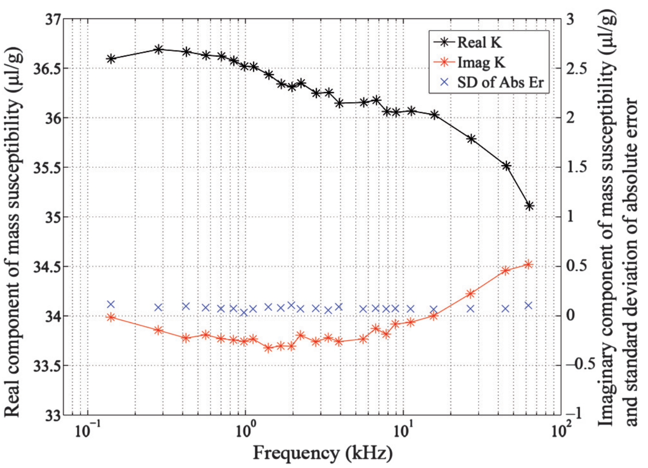

Figure 11. UTEMIS plot of the mass susceptibility for the M1-M2 sample (7.73 g). The negative slope in the real component between 300 Hz and 10 kHz with a nearly constant out-of-phase component suggests a frequency-dependent magnetization. The out-of-phase negative peak at 1.4 kHz indicates a very weak conductive component, suggesting that the overall response is complicated and encompasses induced magnetization and a conductive response. Measurements values greater than 20 kHz may be affected by extraneous sources.

Finally, it should be emphasized that the UTEMIS response obtained from representative rock samples is difficult to interpret because it is often comprised of induced magnetization and a conductive response. For example, Figure 11 shows frequency dependence of the in-phase component, which is superposed on a strong frequency-independent induced magnetization, and the out-of-phase component shows a very weak response. This type of response infers that MV could be interpreted to be present. However, because there is known massive chalcopyrite in the studied sample J, the response could also be explained by its conductive nature. Discriminating between the dispersive rock susceptibility response and very weak conductive mineralization is not obvious on these samples. The same ambiguity exists in the time domain, which is why the MV responses can be misinterpreted as due to conductive bodies. In the time domain, the MV is characterized by a $1/t$ time dependence. In the frequency domain, there might be a comparable characteristic that can be used to identify MV, likely one or more changes in the in-phase component over a broad range of frequencies.

CONCLUSION

Ground TDEM measurements at some stations at Opemiska, Québec, show a slow positive decay inside the loop and a negative decay outside the loop. We have concluded that this is due to MV because the time decay exhibits a power-law decay with the exponent being close to -1, which is consistent with other cases in which there is magnetically viscous material in the subsurface, and it is also consistent with theoretical predictions for MV material.

In other locations in the world, the MV material is believed to be mainly due to maghemite in the weathered regolith or soil. Although further research would be needed to confirm the absence of maghemite in the Opemiska overburden, maghemite is unlikely at Opemiska where there is no regolith; furthermore, in some cases, the MV at Opemiska is measured where there is exposed bedrock. Therefore, a source of MV is directly required from material in the bedrock.

The amplitude of the MV response is more likely exhibited by the presence of extremely fine-grained magnetic material, but it is also a function of the grain shape, the mineralogy, and the time scale, intensity and direction of the external field applied to induce the remanence. Samples collected from the Opemiska area, where MV is measured to show magnetic minerals with grain sizes less than 1 µm, with variable orientations, shapes, and textures.

Material that is magnetically viscous typically shows a magnetic susceptibility that varies as a function of frequency. The UTEMIS measurements of the magnetization as a function of frequency on Opemiska rock samples display a noticeable frequency dependence of the in-phase component with a near zero out-of-phase component. The frequency dependence could be explained by conductive effects, but a relatively large nonzero frequency-independent magnetization implies the material is magnetic, and hence the dispersion is more likely due to MV associated with fine-grained magnetic grains. The magnetic nature is consistent with a certain fraction of coarse-grained magnetic grains that are also seen in the microscopy.

Therefore, we conclude that at Opemiska, the fine fraction of the ferromagnetic grains (such as magnetite, ilmenite, and pyrrhotite) in the bedrock could cause MV and be responsible for the late-time $1/t$ decay observed in the z-component of the TDEM survey carried out in 2015. This conclusion at this site might be applicable at other sites in Canada and Greenland, where MV effects have been observed in airborne EM data and where maghemite in regolith, soils, or clays is unlikely.

ACKNOWLEDGMENTS

We would like to express our gratitude for financial support by the *Natural Sciences and Engineering Research Council* of Canada, Instrumentation GDD Inc., and Explorateurs-Innovateurs de Québec Inc. We gratefully acknowledge the assistance and guidance provided by G. F. West, and the help from B. Polzer to use the electromagnetic induction spectrometer. We also thank A. M. McDonald, W. Zhe, and B. Vandenberg for their expertise and contribution in the use of the SEM. Finally, we also thank A. King, B. Spicer, B. Polzer, P. Gaucher, C. Malo-Lalonde, R. Desbiens, J. Macnae, J. Legault, and D. Sattel for helpful suggestions and careful reviews of the manuscript.

NOMENCLATURE

Mathematical symbols and abbreviations used in the paper

A	=	Ampere
α	=	Alpha parameter
cm	=	Centimeter
I	=	Current (A)
∂	=	Derivative ($\partial B/\partial t$ is the variation of the magnetic field in function of time)
g	=	Gram
Hz	=	Hertz
k	=	Kilo
l	=	Liter
m	=	Magnetance (p_m/H) (µl)
B	=	Magnetic flux density (weber/m^2)
H	=	Magnetic field intensity (A/m)
p_m	=	Magnetic dipole moment (Am^2)
χ	=	Magnetic mass susceptibility (µl/g $= 10^{-6}$ m^3/kg)
M; Ms	=	Magnetization; spontaneous magnetization
m	=	Mass
m	=	Meter
μ	=	Micro (10^{-6})
ml	=	Milliliters
ms	=	Milliseconds
%	=	Percent
t	=	Time
τ	=	Time constant tau
V	=	Voltage

Term and significance

EM	=	Electromagnetic
GDD	=	Acronym for the company name Instrumentation GDD Inc.
GSC	=	Geological Survey of Canada
L	=	Line
MPP	=	Multiparameter probe
MV	=	Magnetic viscosity
PTS	=	Polished thin section
Rx	=	Receiver
SCIP	=	Sample core induced polarization
SEI	=	Scanning electron image
SEM	=	Scanning electron microscope
St.	=	Station
SPM	=	Superparamagnetic
TDEM	=	Time-domain electromagnetic
Tx	=	Transmitter
UTEMIS	=	University of Toronto EM Induction Spectrometer

Abbreviations and chemical formulas of minerals used in the paper (after Kretz, 1983; Lindsley, 1991; Whitney and Evans, 2010)

Au	=	Gold (Au)
Cpy	=	Chalcopyrite ($CuFeS_2$)
Ilm	=	Ilmenite ($FeTiO_3$)
Mgh	=	Maghemite (γ-Fe_2O_3)
Mt	=	Magnetite (Fe_3O_4)
Po	=	Pyrrhotite ($Fe_{1-x}S$)
Py	=	Pyrite (FeS)
Qtz	=	Quartz (SiO_2)

REFERENCES

Anand, R. R., and R. J. Gilkes, 1987, The association of maghemite and corundum in Darling Range laterites, Western Australia: Australian Journal of Soil Research, **25**, 303–311, doi: 10.1071/SR9870303.

Bailey, R. C., and G. F. West, 2007, Project to study soil electromagnetic properties: Defense Research and Defense Canada, Final Report, DRDC Suffield CR 2009-051, No. W7702-03R942/001/EDM.

Barsukov, P. O., and E. B. Fainberg, 1997, Superparamagnetic chimney effect above gold and nickel deposits: Doklady RAN, **353**, 811–814.

Barsukov, P. O., and E. B. Fainberg, 2001, Superparamagnetic effect over gold and nickel deposits: European Journal of Environmental and Engineering Geophysics, **6**, 61–72.

Billings, S., L. Pasion, D. W. Oldenburg, and J. Foley, 2003, The influence of magnetic viscosity on electromagnetic sensors: Proceedings of EUDEM-SCOT2, International Conference on Requirements and Technologies for the detection, removal and neutralization of landmines and UXO.

Bogdanov, A., and A. Y. Vlasov, 1966, On the effect of elastic stresses on the domain structure of magnetite, Izvestiya, Academy of Sciences, U.S.S.R.: Physics of the Solid Earth, **1**, 42–46.

Boyd, J. R., M. Fuller, and S. Halgedahl, 1984, Domain wall nucleation as a controlling factor in the behaviour of fine magnetic particles in rocks: Geophysical Research Letters, **11**, 193–196, doi: 10.1029/GL011i003p00193.

Buselli, G., 1982, The effect of near-surface superparamagnetic material on electromagnetic measurements: Geophysics, **47**, 1315–1324, doi: 10.1190/1.1441392.

Butler, F., and S. K. Banerjee, 1975, Theoretical single-domain grain size range in magnetite and titanomagnetite: Journal of Geophysical Research, **80**, 4049–4058, doi: 10.1029/JB080i029p04049.

Chikazumi, S., and S. H. Charap, 1978, Physics of magnetism: Krieger Publishing Company.

Dabas, M., and J. R. Skinner, 1993, Time-domain magnetization of soils (VRM): Experimental relationship to quadrature susceptibility: Geophysics, **58**, 326–333, doi: 10.1190/1.1443416.

Das, Y., 2005, Electromagnetic induction response of a target buried in conductive and magnetic soil, *in* R. S. Harmon, J. T. Broach, and J. Holloway, eds., Detection and remediation technologies for mines and mine-like targets X: Proceedings of SPIE 5794, 263–274, doi: 10.1117/12.601266.

Dunlop, D. J., 1973, Superparamagnetic and single-domain threshold sizes in magnetite: Journal of Geophysical Research, **78**, 1780–1793, doi: 10.1029/JB078i011p01780.

Dunlop, D. J., 1983, Viscous magnetization of 0.04–100 μm magnetite: Geophysical Journal of the Royal Astronomical Society, **74**, 667–687.

Dunlop, D. J., 1995, Magnetism in rocks: Journal of Geophysical Research, **100**, 2161–2174, doi: 10.1029/94JB02624.

Dunlop, D. J., and Ö. Özdemir, 2001, Rock magnetism: Fundamentals and frontiers: Cambridge University Press.

Dunlop, D. J., and L. D. Schutts, 1979, Fine-particles rock magnetism: Geophysics Laboratory, University of Toronto Annual Report, 36–37.

Fabian, K., and A. Hubert, 1999, Shape-induced pseudo-single-domain remanence: Geophysical Journal, **138**, 717–726, doi: 10.1046/j.1365-246x.1999.00916.x.

Gaucher, F. E. S., 2017, Exploring for copper-gold deposits with electromagnetic surveys at Opemiska, Canada: M.Sc. thesis, Laurentian University.

Graham, J. W., 1953, Changes in ferromagnetic minerals and their bearing on magnetic properties of rocks: Journal of Geophysical Research, **58**, 243–260, doi: 10.1029/JZ058i002p00243.

Halgedahl, S. L., and M. Fuller, 1980, Magnetic domain observations of nucleation processes in fine particles of intermediate titano-magnetite: Nature, **288**, 70–72, doi: 10.1038/288070a0.

Hodych, J., 1977, Single-domain theory for the reversible effect of small uniaxial stress upon the remanent magnetization of rock: Canadian Journal of Earth Sciences, **14**, 2047–2061, doi: 10.1139/e77-175.

Hutchinson, R. W., 1982, Syn-depositional hydrothermal processes and precambrian sulphide deposits, *in* R. W. Hutchinson, C. D. Spence, and J. M. Franklin, eds., Precambrian sulphide deposits, H. S. Robinson Memorial Volume: Geological Association of Canada, Special Paper 25, 761–791.

Julian, S. R., J. A. Westgate, J. M. Daniels, D. G. Rancourt, and P. Sullivan, 1988, A comparison of the titanomagnetites produced by several volcanoes in Iceland: Hyperfine Interactions, **41**, 807–810, doi: 10.1007/BF02400513.

Keating, P., D. Lefebvre, D. Rainsford, and D. Oneschuk, 2010, Geophysical series, parts of NTS 31, 32, 41 and 42, Abitibi greenstone belt, Québec and Ontario: Geological Survey of Canada, Open file 6563; Ministère des Ressources naturelles et de la Faune du Québec, DP-2010-05, 2 cartes: Ontario Geological Survey, Map 81 998, scale 1: 500 000.

Konishi, H., H. Xu, and H. Guo, 2012, Nanostructures of natural iron oxide nanoparticles, *in* A. Barnard and H. Guo, eds., Nature's nanostructures: Pan Stanford Publishing.

Kozhevnikov, N., and E. Antonov, 2011, Magnetic relaxation of a horizontal layer: Effect on TEM data: Russian Geology and Geophysics, **52**, 398–404, doi: 10.1016/j.rgg.2011.03.002.

Kratzer, T., J. Macnae, and P. Mutton, 2013, Detection and correction of SPM effects in airborne EM surveys: Exploration Geophysics, **44**, 6–15, doi: 10.1071/EG12048.

Kretz, R., 1983, Symbols for rock-forming minerals: American Mineralogist, **68**, 227–279.

Lavoie, J. S., 1972, Geology of Opemiska mines, Falconbridge Copper Limited, Opemiska Division: Internal report.

Leclerc, F., P. Houle, and R. Russell, 2009, Géologie de la région de Chapais (32G15-200-0101), RP 2010–09: Ministère des ressources naturelles du Québec.

Lee, T. J., 1978, The effect of loop height in transient electromagnetic modeling or prospecting: Bulletin of the Australian SEG, **9**, 34–35.

Lee, T., 1984a, The effect of a superparamagnetic layer on the transient electromagnetic response of a ground: Geophysical Prospecting, **32**, 480–496, doi: 10.1111/j.1365-2478.1984.tb01111.x.

Lee, T., 1984b, The transient electromagnetic response of a magnetic or a superparamagnetic ground: Geophysics, **49**, 854–860, doi: 10.1190/1.1441731.

Legault, J., K. Kwan, G. Plastow, A. Prikhodko, N. Bournas, M. Orta, and S. Taylor, 2016, Evidence and identification of SPM in airborne TDEM data from Greenland: 86th Annual International Meeting, SEG, Expanded Abstracts, 2195–2199, doi: 101.190/segam2016-13964204.1.

Levi, S., and R. T. Merrill, 1978, Properties of single-domain, pseudo-single-domain, and multidomain magnetite: Journal of Geophysical Research: Solid Earth, **83**, 309–323, doi: 10.1029/JB083iB01p00309.

Lindsley, D. H., 1991, Oxide minerals: Their petrologic and magnetic significance, Review in Mineralogy: Mineralogical Society of America.

Macnae, J., 2016, Definitive superparamagnetic source identification through spatial, spectral, and amplitude analysis of airborne electromagnetic data: Geophysical Prospecting, **65**, 1071–1084, doi: 10.1111/1365-2478.12463.

Mcleod, C. R., 1970, Some Canadian occurrences of maghemite: Geological Survey of Canada, Paper 70-7, doi: 10.4095/102384.

McMillan, R. H., 1972, Petrology, geochemistry and wallrock alteration at Opemiska — A vein copper deposit crosscutting a layered Archean ultramafic-mafic sill: Ph.D. thesis, University of Western Ontario.

Montonen, M., 2015, SPM effect in glacial till: 24th International Geophysical Conference and Exhibition, ASEG, Extended Abstracts, 1–4.

Moskowitz, B. M., R. B. Frankel, P. J. Flanders, R. P. Blakemore, and B. B. Schwartz, 1988, Magnetic properties of magnetotactic bacteria: Journal of Magnetism and Magnetic Materials, **73**, 273–288, doi: 10.1016/0304-8853(88)90093-5.

Mullins, C. E., and M. S. Tite, 1973, Magnetic viscosity, quadrature susceptibility, and frequency dependence of susceptibility in single-domain assemblies of magnetite and maghemite: Journal of Geophysical Research, **78**, 804–809, doi: 10.1029/JB078i005p00804.

Mutton, P., 2012, Superparamagnetic effects in EM surveys for mineral exploration: 22nd International Geophysical Conference and Exhibition, ASEG, Extended Abstracts, 1–6.

Nagata, T., 1961, Rock magnetism: Plenum Press.

Néel, L., 1949, Théorie du traînage magnétique des ferromagnétiques en grains fins avec application aux terres cuites: Annales de géophysique, **5**, 99–136.

Oades, J. M., and W. N. Townsend, 1963, The detection of ferromagnetic minerals in soils and clays: Journal of Soil Science, **14**, 179–187, doi: 10.1111/j.1365-2389.1963.tb00943.x.

Özdemir, Ö., and D. J. Dunlop, 1993, Magnetic domain structures on a natural single crystal of magnetite: Geophysical Research Letters, **20**, 1835–1838, doi: 10.1029/93GL01936.

Parry, L. G., 1965, Magnetic properties of dispersed magnetite powders: Philosophical Magazine, **11**, 303–312, doi: 10.1080/14786436508221858.

Pasion, L. R., S. D. Billings, and D. W. Oldenburg, 2002, Evaluating the effects of magnetic soils on TEM measurements for UXO detection: 72nd Annual International Meeting, SEG, Expanded Abstracts, 1428–1431.

Pawluk, S., 1971, Characteristics of fera eluviated gleysols developed from acid shales in northwestern Alberta: Canadian Journal of Soil Science, **51**, 113–124, doi: 10.4141/cjss71-014.

Raiche, A. P., 1978, The response of a coincident loop transient electromagnetic system above a uniform earth: Bulletin of the ASEG, **9**, 170–172.

Robert, F., 1994, Timing relationships between Cu-Au mineralization, dykes and shear zones in the Chibougamau camp, northeastern Abitibi subprovince, Québec, Current Research: Geological Survey of Canada, 287–294.

Salmon, B., 1982, Distribution de la minéralisation d'une veine cuprifère sur la propriété de Falconbridge Copper Ltée à Chapais, P.Q.: B.ing. thesis report, École Polytechnique de Montréal.

Sattel, D., and P. Mutton, 2014, Modelling the superparamagnetic response of AEM data: Exploration Geophysics, **46**, 118–129, doi: 10.1071/EG14005.

Schlinger, C. M., and R. M. Smith, 1986, Superparamagnetism in volcanic glasses of the KBS Tuff: Transmission electron microscopy and magnetic behavior: Geophysical Research Letters, **13**, 729–732, doi: 10.1029/GL013i008p00729.

Schlinger, C. M., R. M. Smith, and D. R. Veblen, 1986, Geological origin of magnetic volcanic glasses in the KBS tuff: Geology, **14**, 959–962, doi: 10.1130/0091-7613(1986)14<959:GOOMVG>2.0.CO;2.

Schwertmann, U., and H. Fechter, 1984, The influence of aluminium on iron oxides. Part XI: Aluminium-substituted maghemite in soils and its formation: Soil Science Society of America Journal, **48**, 1462–1463, doi: 10.2136/sssaj1984.03615995004800060054x.

Stacey, F. D., 1962, A generalized theory of thermoremanence, covering the transition from single-domain to multi-domain magnetic grains: Philosophical Magazine, **7**, 1887–1900, doi: 10.1080/14786436208213853.

Stacey, F. D., and S. K. Banerjee, 1974, The physical principles of rock magnetism: Elsevier.

Stanjek, H., 1987, The formation of maghemite and hematite from lepidocrocite and goethite in a cambisol from Corsica, France: Journal of Plant Nutrition and Soil Science, **150**, 314–318.

Strangway, D. W., E. E. Larson, and M. Goldstein, 1968, A possible cause of high magnetic stability in volcanic rocks: Journal of Geophysical Research, **73**, 3787–3795, doi: 10.1029/JB073i012p03787.

Tabbagh, A., and M. Dabas, 1996, Absolute magnetic viscosity determination using time-domain electromagnetic devices: Archaeological Prospection, **3**, 199–208, doi: 10.1002/(SICI)1099-0763(199612)3:4<>1.0.CO;2-A.

Taylor, R. M., and U. Schwertmann, 1974, Maghemite in soils and its origin — Properties and observations on soil maghemites: Clay Minerals, **10**, 289–298, doi: 10.1180/claymin.

Van der Marel, H. W., 1951, Gamma ferric oxide in sediments: Journal of Sedimentary Petrology, **21**, 12–21, doi: 10.1306/D42693FF-2B26-11D7-8648000102C1865D.

Van Kampen, N. G., and F. Lurçat, 1961, Causalité et relations de Kramers-Kronig: Journal de physique et le Radium, **22**, 179–191, doi: 10.1051/jphysrad:01961002203017900.

Watkins, D. H., and G. Riverin, 1982, Geology of the Opemiska copper-gold deposits at Chapais, Québec. Precambrian sulphide deposits, *in* R. W. Hutchinson, C. D. Spence, and J. M. Franklin, eds., Precambrian sulphide deposits, H. S. Robinson Memorial Volume: Geological Association of Canada, 427–446.

West, G. F., and S. Holladay, 2014, UTEMIS II operating manual: University of Toronto.

Whitney, D. L., and B. W. Evans, 2010, Abbreviations for names and rock-forming minerals: American Mineralogist, **95**, 185–187, doi: 10.2138/am.2010.3371.

Williams, D., and D. J. Dunlop, 1989, Three-dimensional modeling of ferromagnetic domain structure: Nature, **337**, 634–637, doi: 10.1038/337634a0.

Worm, H.-U., P. J. Ryan, and S. K. Banerjee, 1991, Domain size, closure domains and the importance of magnetostriction in magnetite: Earth and Planetary Science Letters, **102**, 71–78, doi: 10.1016/0012-821X(91)90018-D.

Xu, S., and D. J. Dunlop, 1993, Theory of alternation field demagnetization of multidomain grains and implications for the origins of pseudo-single-domain remanence: Journal of Geophysical Research, **98**, 4183–4190, doi: 10.1029/92JB02570.